forms have often complained that alternative hypotheses of anthropoid origins rely on the assumption that a long interval of anthropoid history remains undocumented paleontologically; that is, that undoubted anthropoids evolved from a poorly known third group of early Cenozoic primates that were neither adapiforms nor omomyids (*17*). We submit that Eosimiidae represent this third group of early Cenozoic primates, amply demonstrating that the anthropoid clade was distinct from both Strepsirhini (including Adapiformes) and Tarsiiformes (including Omomyidae) by the middle Eocene if not earlier.

The fossil record of early anthropoid primates has been greatly augmented in recent years and is now sufficient to demonstrate that by the middle Eocene, higher primates ranged from western Algeria (*2*, *20*) to eastern China. This wide geographic range and the high taxonomic diversity of early anthropoids imply that the anthropoid clade is far more ancient than most workers have assumed. Nevertheless, this great antiquity for the anthropoid clade is consistent with the paleontologically documented antiquity of its likely sister group, the Tarsiiformes (*18*). Robust paleobiogeographic hypotheses regarding the continent of origin for Anthropoidea—either Asia or Africa—must be based on better paleontological data than are currently available.

REFERENCES AND NOTES

1. K. C. Beard, T. Qi, M. R. Dawson, B. Wang, C. Li, *Nature* **368**, 604 (1994).
2. M. Godinot and M. Mahboubi, *C. R. Acad. Sci. Ser. II Mec. Phys. Chim. Sci. Terre Univers.* **319**, 357 (1994); M. Godinot, in *Anthropoid Origins*, J. G. Fleagle and R. F. Kay, Eds. (Plenum, New York, 1994), pp. 235–295.
3. E. L. Simons and D. T. Rasmussen, *Proc. Natl. Acad. Sci. U.S.A.* **91**, 9946 (1994); *Evol. Anthropol.* **3**, 128 (1994).
4. E. L. Simons, *Science* **268**, 1885 (1995).
5. Order Primates, Suborder Anthropoidea, Family Eosimiidae, *Eosimias centennicus*, n. sp. **Holotype**: IVPP V11000, associated left and right dentaries of a single individual preserving right I_1 through M_3 and left C_1 through M_3 (Figs. 2 and 3). Dental measurements (in millimeters) for the right dentary are as follows: I_1 mesiodistal length (L) 0.60, labiolingual width (W) 0.45; I_2 L 0.90, W 0.80; C_1 L 1.70, W 1.40; P_2 L 1.00, W 0.85; P_3 L 1.60, W 1.40; P_4 L 1.70, W 1.45; M_1 L 1.95, W 1.60; M_2 L 1.95, W 1.70; and M_3 L 2.35, W 1.55. **Type locality**: Locality 1, the "River Section" locality of Zdansky (*6*), Zhaili Member, Heti Formation, Yuanqu Basin, Shanxi Province, China (35°04.95′N, 111°50.99′E). **Hypodigm**: The holotype; IVPP V11001.1, right dentary preserving P_3 through M_3; and IVPP V11001.2, right dentary preserving P_4 through M_2. **Known distribution**: Late middle Eocene of Shanxi Province, China. **Diagnosis**: Slightly larger than *E. sinensis*. P_4 differs from that in *E. sinensis* in having a trigonid with a distinct paraconid and a stronger metaconid. The P_4 metaconid is higher and more mesial in position than in *E. sinensis*. **Etymology**: In commemoration of the centennial of the Carnegie Museum of Natural History, celebrated in 1995–96.
6. O. Zdansky, *Palaeontol. Sinica* (ser. C) **6**, 1 (1930).
7. D. E. Russell and R. Zhai, *Mem. Mus. Natl. Hist. Nat. Ser. C. Geol.* **52**, 1 (1987); Y. Tong, *Acta Palaeontol. Sinica* **28**, 663 (1989); P. A. Holroyd and R. L. Ciochon, in *Anthropoid Origins*, J. G. Fleagle and R. F. Kay, Eds. (Plenum, New York, 1994), pp. 123–141.
8. Y. Tong, *Vertebr. Palasiat.* **30**, 1 (1992).
9. B. Wang and M. R. Dawson, *Ann. Carnegie Mus.* **63**, 239 (1994).
10. H. H. Covert and B. A. Williams, *J. Hum. Evol.* **21**, 463 (1991); ———, in *Anthropoid Origins*, J. G. Fleagle and R. F. Kay, Eds. (Plenum, New York, 1994), pp. 29–54.
11. D. T. Rasmussen, M. Shekelle, S. L. Walsh, B. O. Riney, *J. Hum. Evol.* **29**, 301 (1995).
12. T. M. Bown and K. D. Rose, *Paleontol. Soc. Mem.* **23**, 1 (1987).
13. K. D. Rose and T. M. Bown, *Proc. Natl. Acad. Sci. U.S.A.* **88**, 98 (1991); K. D. Rose, M. Godinot, T. M. Bown, in *Anthropoid Origins*, J. G. Fleagle and R. F. Kay, Eds. (Plenum, New York, 1994), pp. 1–28.
14. G. C. Conroy, *Int. J. Primatol.* **8**, 115 (1987).
15. R. F. Kay and H. H. Covert, in *Food Acquisition and Processing in Primates*, D. J. Chivers, B. A. Wood, A. Bilsborough, Eds. (Plenum, New York, 1984), pp. 467–508.
16. P. D. Gingerich, *Contrib. Mus. Paleontol. Univ. Mich.* **24**, 163 (1975); *Geobios Mem. Spec.* **1**, 165 (1977).
17. D. T. Rasmussen, in *Anthropoid Origins*, J. G. Fleagle and R. F. Kay, Eds. (Plenum, New York, 1994), pp. 335–360; P. D. Gingerich, P. A. Holroyd, R. L. Ciochon, *ibid.*, pp. 163–177.
18. R. Hoffstetter, *Bull. Mem. Soc. d'Anthrop. Paris* (ser. XIII) **4**, 327 (1977); K. C. Beard, L. Krishtalka, R. K. Stucky, *Nature* **349**, 64 (1991); K. C. Beard and R. D. E. MacPhee, in *Anthropoid Origins*, J. G. Fleagle and R. F. Kay, Eds. (Plenum, New York, 1994), pp. 55–97.
19. R. D. Martin, *Primate Origins and Evolution: A Phylogenetic Reconstruction* (Chapman and Hall, London, 1990).
20. M. Godinot and M. Mahboubi, *Nature* **357**, 324 (1992).

21. We thank J. Kappelman, W. Gose, T. Ryan, and J. Guo for aiding us in the field and C. R. Schaff and A. R. Tabrum for fossil preparation. Financial support from the L. S. B. Leakey Foundation, the National Geographic Society, NSF, and the Carnegie Museum of Natural History is gratefully acknowledged.

20 December 1995; accepted 23 January 1996

Imprint Lithography with 25-Nanometer Resolution

Stephen Y. Chou,* Peter R. Krauss, Preston J. Renstrom

A high-throughput lithographic method with 25-nanometer resolution and smooth vertical sidewalls is proposed and demonstrated. The technique uses compression molding to create a thickness contrast pattern in a thin resist film carried on a substrate, followed by anisotropic etching to transfer the pattern through the entire resist thickness. Metal patterns with a feature size of 25 nanometers and a period of 70 nanometers were fabricated with the use of resist templates created by imprint lithography in combination with a lift-off process. With further development, imprint lithography should allow fabrication of sub–10-nanometer structures and may become a commercially viable technique for manufacturing integrated circuits and other nanodevices.

The development of low-cost, high-throughput lithography techniques with sub–50-nm linewidth resolution is essential for the future manufacturing of semiconductor integrated circuits and the commercialization of electronic, optoelectronic, and magnetic nanodevices. Numerous technologies are under development. Scanning electron beam lithography has demonstrated 10-nm resolution (*1*); however, because it exposes point by point in a serial manner, the current throughput of the technique is too low to be economically practical for mass production of sub–50-nm structures. X-ray lithography has demonstrated 20-nm resolution (*2*) in a contact printing mode and can have a high throughput, but its mask technology and exposure systems are currently rather complex and expensive. Lithographies based on scanning proximal probes, which have shown a resolution of about 10 nm, are in the early stages of development (*3*).

NanoStructure Laboratory, Department of Electrical Engineering, University of Minnesota, Minneapolis, MN 55455, USA.

*To whom correspondence should be addressed. E-mail: chou@ee.umn.edu

In this report, we demonstrate an alternative lithographic method, imprint lithography, that is based on compression molding and a pattern transfer process. Compression molding is a low-cost, high-throughput manufacturing technology that has been in use for decades and features with sizes of >1 μm are routinely imprinted in plastics. Compact disks based on imprinting in polycarbonate are one example. Other examples are imprinted polymethylmethacrylate (PMMA) structures with a feature size on the order of 10 μm (*4*) and imprinted polyester patterns with feature dimensions of several tens of micrometers (*5*). However, compression molding has not been developed into a lithographic method to pattern semiconductors, metals, and other materials used in semiconductor integrated circuit manufacturing.

Using imprint lithography, we achieved a minimum feature size of 25 nm and a period of 70 nm in a resist >100 nm thick. We then fabricated 25-nm metal patterns by means of imprint lithography and a lift-off process. We believe that with further development, imprint lithography may become a commercially viable lithography

technique for manufacturing integrated circuits and other sub–50-nm structures.

In imprint lithography, a mold with nanometer-scale features is first pressed into a thin resist cast on a substrate, which creates a thickness contrast pattern in the resist (Fig. 1). After the mold is removed, an anisotropic etching process is used to transfer the pattern into the entire resist thickness by removing the remaining resist in the compressed areas. Preferably, the resist is a thermoplastic polymer that is heated during the molding step to soften the polymer relative to the mold. If the temperature is above the polymer's glass transition temperature, the polymer behaves as a viscous liquid and can flow, thereby conforming to the mold. The mold can be made of metals, dielectrics, or semiconductors. Reactive ion etching (RIE), wet etching, and other processes can be used to transfer the thickness contrast pattern created by imprinting through the entire resist thickness.

Our experiments used silicon dioxide molds on a silicon substrate. The mold was patterned with dots and lines with a minimum lateral feature size of 25 nm by means of electron beam lithography, and the patterns were etched into the SiO_2 layer by fluorine-based RIE. The thin resist used for imprint lithography was a PMMA polymer spun on a silicon wafer. The PMMA was made in-house to have two desired properties. First, PMMA does not adhere to the SiO_2 mold; good mold release properties are essential for fabricating nanometer-scale features. Second, the shrinkage of PMMA is <0.5% over large ranges of temperature and pressure (6). The thickness of the PMMA varied from 50 to 200 nm, depending on the desired minimum feature size. After imprinting, oxygen RIE was used to anisotropically remove the remaining thin resist layer in the compressed areas, thereby transferring the thickness contrast pattern into the entire resist thickness.

In the imprinting step of imprint lithography, both the mold and PMMA were first heated to 200°C, above the glass transition temperature of PMMA, 105°C. The mold was then pressed against the sample and held there until the temperature dropped below the PMMA's glass transition temperature. Various pressures were tested and it was found that the optimum pressure was about 13 MPa. At that pressure, the pattern on the mold could be fully transferred into the PMMA over the entire 4-cm^2 sample.

Examples of imprinted PMMA structures before oxygen RIE pattern transfer are shown in Figs. 2 to 4. They include holes 25 nm in diameter with a period of 120 nm (Fig. 2), trenches 100 nm wide with a period of 250 nm (Fig. 3), and a perspective view of the sidewalls of PMMA strips 70 nm wide and 200 nm tall (Fig. 4). These micrographs, produced by scanning electron microscopy (SEM), clearly show that the imprinted PMMA structures not only have 25-nm feature size and a high aspect ratio, but also have smooth surfaces with a roughness of <3 nm and corners with nearly perfect 90° angles. Such smoothness, sharp corners, and high aspect ratios at the 70-nm feature size cannot be obtained directly with conventional lithographies. In addition, 30-nm-wide trenches with a 70-nm period were patterned in the PMMA by means of imprint lithography but could not be examined by SEM without severe electron beam–induced melting. The dimensions of these strips were studied by copying the structure into metal (using a lift-off process), as discussed below. The mold had additional features as large as tens of micrometers, which were imprinted nearly perfectly into the PMMA together with the nanometer-scale features.

We also examined the molds with SEM. Comparing the features on the SiO_2 mold with the features imprinted in the PMMA, we could not detect any size difference between the two, which indicated that the imprinted features conformed with the mold. Moreover, sub–10-nm vari-

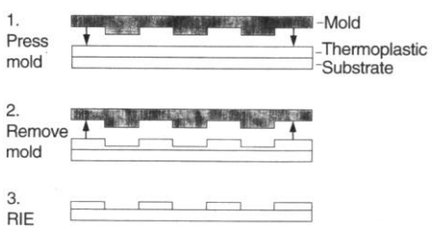

Fig. 1. Schematic of the nanoimprint lithography process. Compression molding is used to create a thickness contrast in a resist, and then anisotropic etching exposes the surface of the underlying substrate.

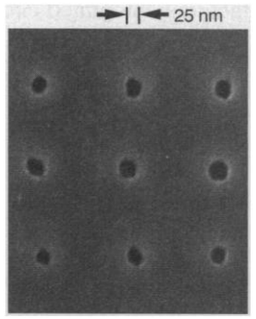

Fig. 2. SEM micrograph of a top view of holes 25 nm in diameter with a period of 120 nm, formed by compression molding into a PMMA film.

Fig. 3. SEM micrograph of a top view of trenches 100 nm wide with a period of 250 nm, formed by compression molding into a PMMA film.

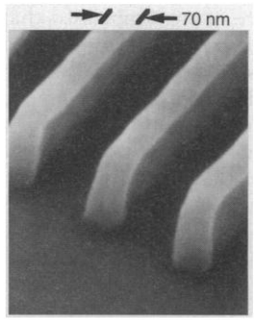

Fig. 4. SEM micrograph of a perspective view of strips formed by compression molding into a PMMA film. The strips, 70 nm wide and 200 nm tall, have a high aspect ratio, a surface roughness of <3 nm, and nearly perfect 90° corners.

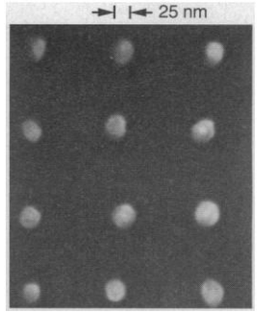

Fig. 5. SEM micrograph of the substrate in Fig. 2, after deposition of metal and a lift-off process. The diameter of the metal dots is 25 nm, the same as that of the original holes created in the PMMA.

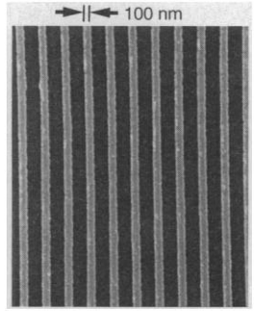

Fig. 6. SEM micrograph of the substrate in Fig. 3, after deposition of metal and a lift-off process. The metal linewidth is 100 nm, the same as the width of the original PMMA trenches.

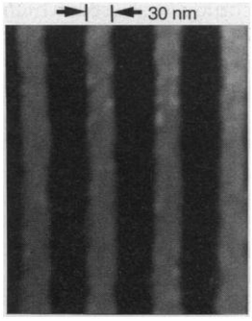

Fig. 7. SEM micrograph of metal lines fabricated by imprint lithography and a lift-off process. The lines are 30 nm wide and have a period of 70 nm.

ations on the mold sidewall could be faithfully imprinted into the PMMA; this observation showed that the minimum linewidth that can be achieved with imprint lithography is limited by mold size. With a suitable mold, 10-nm-wide PMMA lines or trenches may be fabricated by means of imprint lithography.

To examine the extent to which the oxygen RIE pattern transfer step removed the residual resist in the compressed areas and changed the lateral dimension of the PMMA features, we used the PMMA resist structures created by imprint lithography as the template for a lift-off of metals. In the lift-off process, 5 nm of Ti and 15 nm of Au were first deposited onto the entire sample, and then the metal on the PMMA surface was removed when the PMMA was dissolved in acetone. We compared the SEM image of the imprinted PMMA template before the oxygen RIE transfer to that of the metal patterns after the lift-off. SEM micrographs of the metal dots (Fig. 5) and lines (Fig. 6) that were fabricated with the PMMA templates shown in Figs. 2 and 3, respectively, show that the lift-off metal has the same feature size as the original molded PMMA structures. Hence, during the oxygen RIE process, the compressed PMMA area was completely removed and the lateral size of the PMMA features did not change noticeably. Finally, we used imprint lithography and lift-off to fabricate 30-nm-wide metal lines with a 70-nm period (Fig. 7). This SEM micrograph indicates that although the PMMA template cannot be directly seen with SEM because of electron beam–induced melting, 30-nm-wide trenches with a 70-nm period were indeed made in PMMA by means of imprint lithography.

Imprint lithography offers many advantages over conventional lithographies. First, imprint lithography abandons the use of an energetic beam of electrons, photons, or ions, which creates a chemical structure contrast in a resist. Instead, imprint lithography uses compression molding to create a thickness contrast in a resist. As a result, imprint lithography eliminates many factors that limit the resolution of conventional lithographies, such as wave diffraction, scattering in the resist, backscattering from substrate, and chemistry of resists and developers. Second, imprint lithography not only can have 25-nm resolution, but also can print a large area at once, therefore offering a high throughput. Third, its cost is potentially low because it does not require a sophisticated energetic beam generator. We believe that with further development, such as optimization of the polymer resist and mold materials and of the compression conditions, large areas (greater than 50 mm by 50 mm) of sub–25-nm imprint lithography should be achievable without the sticking and defect problems associated with traditional contact printing. These developments would make imprint lithography a viable technology for manufacturing 25-nm structures.

REFERENCES AND NOTES

1. A. N. Broers, J. M. Harper, W. W. Molzen, *Appl. Phys. Lett.* **33**, 392 (1978); P. B. Fischer and S. Y. Chou, *ibid.* **62**, 2989 (1993).
2. D. Flanders, *ibid.* **36**, 93 (1980); K. Early, M. L. Schattenburg, H. I. Smith, *Microelectron. Eng.* **11**, 317 (1990).
3. M. A. McCord and R. F. P. Pease, *J. Vac. Sci. Technol.* **B4**, 86 (1986); J. W. Lyding, T. C. Shen, J. S. Hubacek, J. R. Tucker, G. C. Abelin, *Appl. Phys. Lett.* **64**, 2010 (1994); N. Kramer, M. Birk, J. Jorvitsma, C. Schronenberger, *ibid.* **66**, 1325 (1995).
4. M. Harmening *et al.*, *Proceedings IEEE Micro Electro Mechanical Systems* (IEEE, Piscataway, NJ, 1992), p. 202.
5. H. Li and S. D. Senturia, *Proceedings of the 13th IEEE/CHMT International Electronic Manufacturing Technology Symposium* (IEEE, Piscataway, NJ, 1992), p. 145.
6. I. Rubin, *Injection Molding* (Wiley, New York, 1972).

7. We thank other members of the NanoStructure Laboratory whose efforts have profoundly affected the current work. S.Y.C. thanks W. T. Peria for suggesting the term thickness-contrast lithography as an alternative name for imprint lithography. Supported in part by the Packard Foundation through a Packard fellowship.

12 December 1995; accepted 12 February 1996

Autocatalysis During Fullerene Growth

B. R. Eggen,* M. I. Heggie, G. Jungnickel, C. D. Latham, R. Jones, P. R. Briddon

Total energy calculations with a local spin density functional have been applied to the Stone-Wales transformation in fullerene (C_{60}). In the formation of the almost exclusively observed I_h isomer of C_{60} with isolated pentagons, the final transformation must be from a C_{2v} isomer with two pentagon pairs. It was found that the energy barrier for this rearrangement was substantially reduced in the presence of an extra carbon atom. Such atoms were found to bind loosely, preferentially to regions in which there were paired pentagons. Pentagon rearrangements, which are necessary steps in the growth of fullerenes, may therefore result from autocatalysis by carbon.

One of the great surprises in fullerene chemistry has been that only one isomer of C_{60} is isolated in macroscopic quantities—that having I_h symmetry and hence satisfying the isolated pentagon rule (*1*). Evidence for defect isomers is scarce, although they have been observed with scanning-tunneling microscopy (*2*). Whereas this can be understood in broad terms on energetic grounds (*1*)—the observed structure is undeniably the lowest energy isomer—other isomers have energies within 1.5 eV of it, and it is not evident that this energy difference alone would rule out their occurrence in observable quantities. The energy difference is only 0.03 eV per atom, a value similar to the difference in cohesive energy between diamond and graphite (*3*), which does not preclude the existence of diamond as a kinetically stable phase. Furthermore, C_{60} isomers are most likely to interconvert through the Stone-Wales (SW) (*4*) (also known as pyracylene) transformations (Fig. 1), which have been shown by reliable theoretical methods to give rise to extremely high-energy barriers of 6 to 7 eV (*5*–*8*). The C_{2v} C_{60} isomer with two adjacent pentagon pairs is a bottleneck in the SW transformations scheme that connects most of the possible C_{60} isomers, because any SW route to the I_h C_{60} fullerene has to encounter it in the ultimate step (*9*); this last step is the subject of this report.

We have shown that interaction between C_{60} and H can cause the I_h C skeleton to be higher in energy than a D_{6h}

B. R. Eggen and M. I. Heggie, School of Chemistry and Molecular Sciences, University of Sussex at Brighton, Falmer, BN1 9QJ, UK.
G. Jungnickel, Institut für Physik, Theoretische Physik III, Technische Universität Chemnitz-Zwickau, D-09107 Chemnitz, Germany.
C. D. Latham and R. Jones, Department of Physics, University of Exeter, Exeter, EX4 4QL, UK.
P. R. Briddon, Department of Physics, University of Newcastle, Newcastle, NE1 7RU, UK.
*To whom correspondence should be addressed.